Journal of Nuclear Materials 390–391 (2009) 891–894

Contents lists available at ScienceDirect

Journal of Nuclear Materials

journal homepage: www.elsevier.com/locate/jnucmat

Design, R&D and assessment of performance of the JT-60SA upper divertor

Shinji Sakurai *, Hisato Kawashima, Satoru Higashijima, Katsuhiro Shimizu, Kei Masaki, Nobuyuki Asakura, Yusuke K. Shibama, Akira Sakasai

Japan Atomic Energy Agency, Japan

ARTICLE INFO

PACS:
52.55F
52.65

ABSTRACT

Modification of JT-60 to a fully superconducting coil tokamak (JT-60 Super Advanced) has been started last year. Divertor plasma performance for high triangularity and low aspect ratio plasma in two types of divertor geometries was studied and compared by using 2D plasma fluid (SOLDOR) and neutral Monte-Carlo (NEUT2D) codes. 'Vertical target with deep V corner' is effective to reduce heat flux even in low density operation without additional gas puffing, but large pumping speed is required to change particle balance. On the other hand, the particle balance in 'W-shaped with shallow V' can be changed with small pumping speed and larger main plasma can be obtained due to its compactness. Performance of water-cooled mono-block carbon fiber composite (CFC) divertor target has been confirmed by heat load cycle test of small mockup. Obvious performance degradation was not found during 1450 cycles at 15 MW m^{-2} and 600 cycles at 20 MW m^{-2}.

1. Introduction

Modification program of JT-60 to a fully superconducting coil tokamak (JT-60 Super Advanced, JT-60SA) has been started last year. JT-60SA program is a combined program of Japan-EU satellite tokamak program under the Broader Approach (BA) Program and Japan Atomic Energy Agency (JAEA)'s program for national use with equal operating opportunity between the two programs [1].

JT-60SA allows exploration of configuration optimization for ITER and DEMO with a wide variety of plasma shape (elongation κ and triangularity δ) and aspect ratio ($A = R_p/a_p$ down to 2.6) including that of ITER-like and double null configuration. ITER relevant plasma regimes far exceeding the H-mode power threshold can be studied with high power heating. A water-cooled divertor compatible with the maximum heat flux of 15 MW m^{-2} should be required [2]. A remote handling system is equipped to maintain in-vessel components under high dose rate environment due to a substantial annual neutron production. Divertor plasma performance for ITER-like LSN configuration has been studied by using 2D plasma fluid (SOLDOR) and neutral Monte-Carlo (NEUT2D) codes [3,4]. It was confirmed that the combination of (1) vertical outer divertor target, (2) 'V corner' near the strike point and (3) connecting and pumping inner and outer divertor through private region is effective for heat load reduction by partial detachment [5,6].

This paper presents assessment of divertor plasma performance for DEMO-like configuration by using SOLDOR/NEUT2D code and brief summary of design and R&D for divertor components.

2. Requirements of a divertor in JT-60SA

Requirements of a divertor for DEMO-oriented research in JT-60SA are as follows. (1) Divertor geometry should be compatible with high κ, high δ and low A plasma configuration under the limitation of vacuum vessel and divertor cassette geometry. (2) Heat reduction with partial detachment and particle exhaust for density control in high power heated plasma with duration of 100 s are required. Therefore, cryopanels will be installed behind the divertor cassette to obtain enough particle exhaust. (3) 15 MW m^{-2} of heat flux should be removed with a water-cooled divertor target for high power heated plasma operation. (4) Divertor components should be remotely maintained due to high dose rate by a system involving a divertor cassette similar to the ITER. Divertor geometry and cassette structure should allow access to the fixing structure and coolant pipe connection from the front (plasma) side, because JT-60SA does not have large divertor port for maintenance. (5) Flexibility in plasma facing materials for plasma material interaction research toward DEMO. Therefore, an armor tile bolted on a cooled heatsink will be installed except for divertor targets.

3. Assessment of divertor performance

Two types of divertor geometry are considered as an upper divertor for the DEMO-like configuration. Fig. 1(a) shows the

* Corresponding author. Address: 801-1, Mukoyama, Naka-shi, Ibaraki-ken 311-0193, Japan.
E-mail address: sakurai.shinji@jaea.go.jp (S. Sakurai).

0022-3115/$ - see front matter © 2009 Elsevier B.V. All rights reserved.
doi:10.1016/j.jnucmat.2009.01.229

'W-shaped' divertor similar to the present JT-60U, which can allow high κ and low A plasma configurations and channel 2-cm wide SOL to the outer target for avoiding recycling enhancement out of divertor region. The heat reduction of this concept might be insufficient in spite of the 'shallow V corner' for recycling enhancement. Fig. 1(b) shows the 'vertical target with deep V corner' divertor, which might be effective at reducing heat load. However, position of divertor and X-point should be shifted downward ~7 cm to avoid interference between divertor cassette and vacuum vessel. Therefore, allowable elongation and aspect ratio are slightly degraded.

Divertor plasma parameters in the two types of divertor geometry have been evaluated with SOLDOR/NEUT2D. Radiation power from carbon impurity is calculated by a simple non-corona model, assuming residence parameter of $n_e\tau_{res} = 4 \times 10^{15}$ sm^{-3}, where τ_{res} is the impurity residence time in the plasma, and a uniform carbon fraction of 1% of deuterium density in SOL and divertor plasma. Core plasma boundary is set on $r/a = 0.95$, where power flux of 37 MW and ion flux of 5×10^{21} D s^{-1} are exhausted. Neutral particles are fueled from outboard of main plasma when additional gas puffing is applied. The pumping speed of cryopanels is specified at an albedo including transparency of the chevron and exhaust holes in divertor cassette in front of the cryopanel. The recycling coefficient of deuterium is set to unity at all first wall surfaces. Electron and ion thermal diffusivities are assumed to be 1 m^2 s^{-1} at whole edge plasma. Particle diffusion coefficient of 0.3 m^2 s^{-1} is assumed.

Divertor plasma parameters and heat flux profiles along with an outer divertor target without additional gas puffing are shown in Figs. 2 and 3. Higher density, lower temperature and lower peak heat flux are obtained in the 'vertical target with deep V corner' divertor as expected. Peak heat flux can be reduced to 12 MW m^{-2} in the 'vertical target with deep V corner' divertor even without additional gas puffing in comparison with 17 MW m^{-2} in the 'W-shaped with shallow V corner'. It is also confirmed that moderate additional gas puffing of 5×10^{21} D s^{-1} can reduce the peak heat fluxes on the outer divertor target to 11 MW m^{-2} and 5 MW m^{-2} in the 'W-shaped with shallow V corner' and 'vertical target with deep V corner', respectively.

Fig. 4 shows neutral particle balance in the divertor region in both two types of divertor geometry with 5×10^{21} D s^{-1} of additional gas puffing and 50 m^3 s^{-1} of pumping speed. Recycling fluxes from divertor target are similar in both cases. Net particle fluxes are pumped at the inner divertor and fueled at the outer divertor in both cases. However, net fueling fluxes at the outer divertor in the 'vertical target with deep V corner' are about half that for the 'W-shaped with shallow V corner'. Neutral particle controllability in both geometries was compared by changing pumping speed as shown in Table 1. Detachment at the outer divertor is obtained at $\sim 7 \times 10^{23}$ D s^{-1} of recycling flux in both geometries. However, about a half of the net fueling flux can make detachment in the 'vertical with deep V corner' case. On the other hand, neutral particle fluxes through pumping slot at the outer divertor in the 'W-shaped with shallow V corner' are large and sensitively changes with pumping speed.

The 'vertical target with deep V corner' is effective at reducing heat flux even in low density operation without additional gas puffing, but the 'W-shaped with shallow V' design easily control particle balance with small change in pumping speed. The effects of inclination of divertor target and depth of 'V corner' has not been independently clarified yet. Therefore, confirmation and optimization of these effects will be required to fix the design.

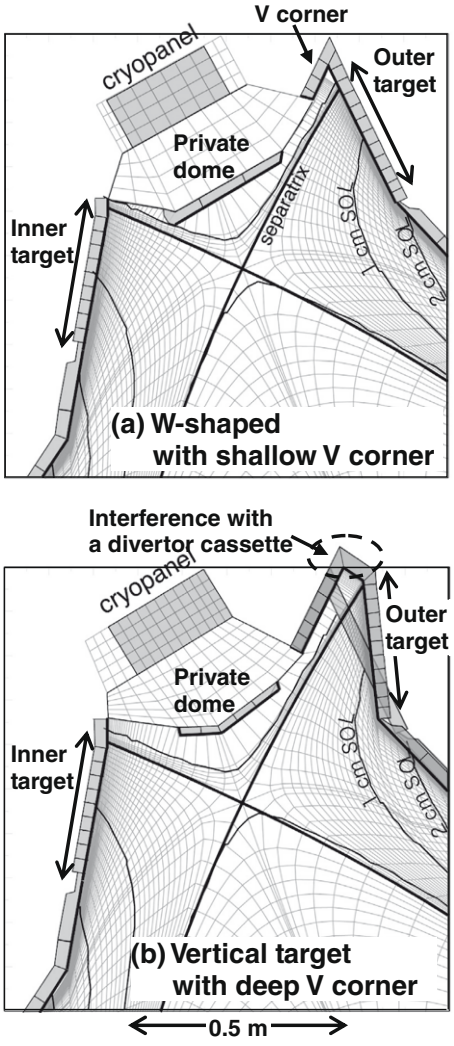

Fig. 1. Divertor geometries for DEMO-oriented research.

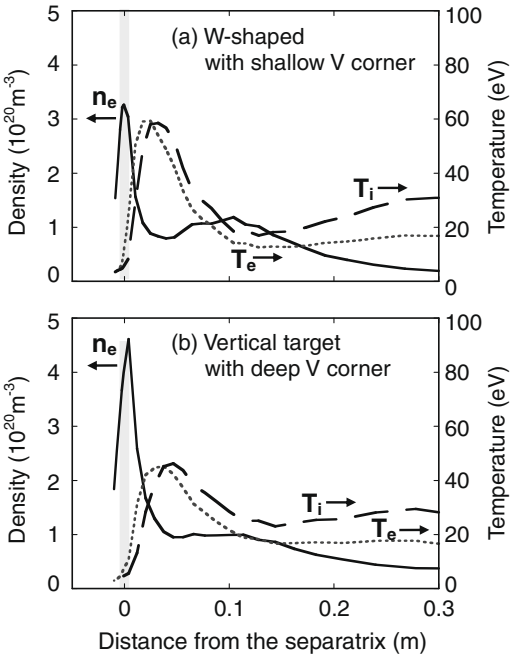

Fig. 2. Electron density n_e, electron and ion temperature T_e, T_i on the outer divertor target. Pumping speed of cryopanel is 50 m^3 s^{-1} without additional gas puffing.

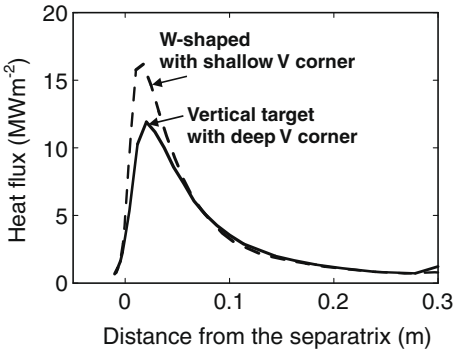

Fig. 3. Heat flux on the outer divertor target. Pumping speed is 50 $m^3 s^{-1}$ without additional gas puffing.

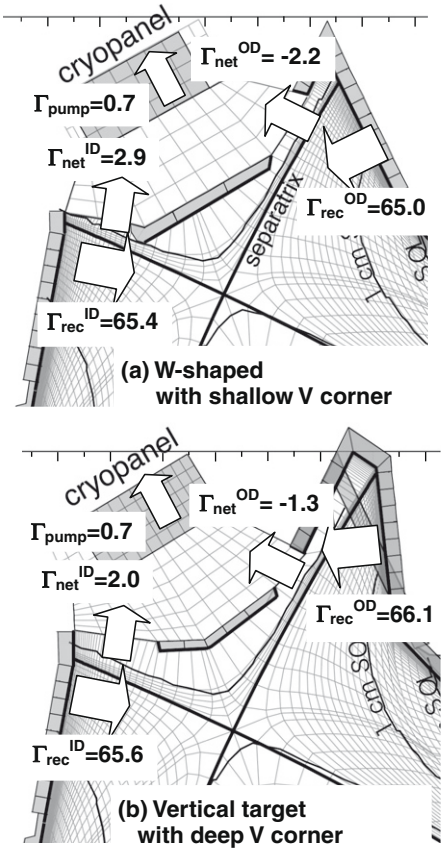

Fig. 4. Neutral particle balance in two types of divertor geometry. Pumping speed of cryopanel is 50 $m^3 s^{-1}$ with additional gas puffing of 5×10^{21} D s^{-1}.

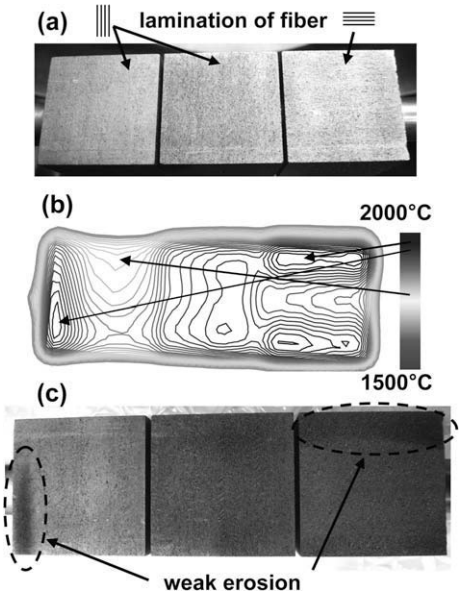

Fig. 5. (a) Small mockup of CFC mono-block target before heat load test. (b) Surface temperature measured by IRTV at 15 MW m^{-2}. (c) Small mockup after heat load test at 15 MW $m^{-2} \times 1350$ cycles and 20 MW $m^{-2} \times 600$ cycles.

4. Design and R&D of divertor components

Water-cooled brazed carbon fiber composite (CFC) targets are planned for the inner and outer divertor targets. Bolted armor tiles on water-cooled heatsink, which give the flexibility to change armor materials, are proposed for the private dome and baffles. All of these plasma facing components are mounted on a divertor cassette, which can be carried out through large horizontal port of a vacuum vessel by remote handling system similar with blanket remote handling system in ITER. Fixing structures and coolant pipe connections can be accessed from plasma side after removing some bolted armor tiles by small manipulator.

Expected heat flux on the outer divertor target exceeds 10 MW m^{-2} as shown in previous section. Outer divertor target should have maximum power handling capability consistent with the R&D for the ITER divertor [7]. A mono-block type CFC target is the most promising candidate to handle heat flux >10 MW m^{-2}. Brazing technique between CFC and copper has been improved by pre-processing on the CFC side for mass production. Fig. 5 showed small mockup for heat load testing by electron beam irradiation. Direction of fiber lamination in 2-D felt CFC of the right block is changed to confirm strength of brazing. Thermal conductivities in the plane of fiber lamination layer 390 W $m^{-1} K^{-1}$ (RT) in comparison with 190 W $m^{-1} K^{-1}$ (RT) in the perpendicular direction. Surface temperature at 15 MW m^{-2} reaches ~2000 °C. High temperature regions due to the direction of fiber lamination and the left edge of the mockups can be seen in the IRTV image. High

Table 1
Comparison of particle balance in two types of divertor geometry with changing pumping speed.

Pumping speed ($m^3 s^{-1}$)	W-shaped with shallow V (D 10^{22} s^{-1})				Outer divertor	Vertical target with deep V (D 10^{22} s^{-1})				Outer divertor
	Γ_{rec}^{ID}	Γ_{net}^{ID}	Γ_{rec}^{OD}	Γ_{net}^{OD}		Γ_{rec}^{ID}	Γ_{net}^{ID}	Γ_{rec}^{OD}	Γ_{net}^{OD}	
30	60.5	3.0	70.3	−2.3	Detach					
40	62.5	2.8	66.6	−2.2	Attach					
50	65.4	2.9	65.0	−2.2	Attach	65.6	2.0	66.1	−1.3	Detach
100						70.0	1.6	67.7	−1.0	Detach
200						72.1	1.5	56.0	−0.9	Attach

temperature at the left edge might be due to electron beam profile because no deep defect was found at the left edge by cutting inspection after heat load test. Obvious increase in surface temperature profile was not found during more than 1450 cycles at 15 MW m^{-2} and 600 cycles at 20 MW m^{-2}. After the heat load test, the surfaces showed slightly eroded regions due to sublimation corresponding to high temperature regions. Performance of the mono-block CFC target with an improved brazing technique allowing 15 MW m^{-2} of heat load has been confirmed. Qualification for mass production with mockups with actual target length is in progress now.

5. Summary

JT-60SA allows exploration of configuration optimization for ITER and DEMO with a wide variety of plasma shape and aspect ratio including that of ITER and a double null configuration with high power long pulse heating. Divertor plasma performance for DEMO-like configuration in two types of divertor geometries was studied and compared by using the SOLDOR/NEUT2D code. The 'vertical target with deep V corner' configuration is effective at reducing at heat flux even in low density operation without additional gas puffing, but it needs more divertor space and slightly degrades elongation and aspect ratio of main plasma. On the other hand, the 'W-shaped with shallow V' design easily controls particle balance with small changes in pumping speed, but the heat reduction is insufficient in low density operation. Effects of inclination of divertor target and depth of 'V corner' has not been independently clarified yet. Therefore, confirmation and optimization of these effects will be required.

Water-cooled brazed CFC targets and bolted armor tiles on water-cooled heatsinks for the private dome and baffles are mounted on a divertor cassette, which can be maintained and exchanged by remote handling system. The performance of a mono-block CFC target with improved brazing technique allowing 15 MW m^{-2} of heat load has been confirmed by heat load cycle test. Qualification for mass production of components with realistic dimensions is in progress now.

References

[1] M. Kikuchi, JA-EU satellite tokamak working group and JT-60SA design team, in: Proceedings of 21st IAEA Fusion Energy Conference, Chengdu, China, 2006, IAEA-CN-149/FT/2-5.
[2] S. Sakurai, K. Masaki, Y.K. Shibama, et al., Fus. Eng. Des. 82 (2007) 1767.
[3] K. Shimizu, T. Takizuka, S. Sakurai, et al., J. Nucl. Mater. 313–316 (2003) 1277.
[4] H. Kawashima, K. Shimizu, T. Takizuka, et al., Plasma Fus. Res. 1 (2006) 031.
[5] N. Asakura, H. Kawashima, K. Shimizu, et al., in: Proceedings of 34th EPS conference on Plasma Physics and Controlled Fusion, Warsaw, Poland, 2007, P1-051.
[6] H. Kawashima, K. Shimizu, T. Takizuka, et al., Fus. Eng. Des., 83 (2008) 1643..
[7] K. Ezato, M. Dairaku, M. Taniguchi, K. Sato, S. Suzuki, M. Akiba, et al., Fus. Sci. Technol. 46 (2004) 530.